JOURNAL OF COMPUTATIONAL PHYSICS 64, 161–176 (1986)

Direct Determination of Axisymmetric Magnetohydrodynamic Equilibria in Hamada Coordinates

GLENN BATEMAN* AND ROBIN G. STORER

School of Physical Sciences, The Flinders University of South Australia, Bedford Park, S.A. 5042, South Australia

Received June 13, 1984; revised May 1, 1985

A direct method has been developed to find axisymmetric magnetohydrodynamic (MHD) equilibria in Hamada coordinates. The problem is reduced to a system of ordinary differential equations for poloidal Fourier harmonics of the spatial coordinates of flux surfaces as functions of Hamada coordinates. These can be used to obtain metric tensor elements and magnetic field components as functions of Hamada coordinates, suitable for direct input into stability or transport codes. Equilibria with prescribed outer boundary shape can be found, given a suitable pair of plasma profiles, such as the pressure and safety factor as functions of poloidal flux.

1. INTRODUCTION

Studies of magnetohydrodynamic stability and transport are often facilitated by the use of a flux coordinate system in which one of the coordinates is constant over each flux surface [1–11]. For axisymmetric toroidal plasmas the starting point of many such calculations is the determination of the solution to the MHD equilibrium equation $\nabla p = \mathbf{J} \times \mathbf{B}$, followed by a mapping procedure which expresses this solution in terms of flux coordinates [10, 11]. Recently, however, several techniques have been developed in which the flux coordinates can be obtained directly [12–15, 20]. The variational methods are useful in situations where it is not necessary to prescribe the form of the Jacobian or to use a coordinate system with straight magnetic field and current density lines.

Hamada coordinates are widely used in the theory of MHD instabilities of toroidal plasmas [1–9, 16]. In this coordinate system the lines of magnetic field and current density both appear to be straight (their contravariant components are uniform over each magnetic surface) and the Jacobian is uniform over each magnetic surface. These features lead to a more straightforward and accurate representation of the partial differential operators used in stability analysis. In the original definition of Hamada coordinates [1, 2] the Jacobian was taken to be

* Permanent address: Plasma Physics Laboratory, Princeton, N.J. 08544.

0021-9991/86 $3.00

unity throughout the domain. However, the essential features of Hamada coordinates are retained if we choose the Jacobian to be a function of the flux coordinate V alone. The derivation can be modified for a Jacobian equal to unity or for other choices of Jacobian, if desired.

In numerical work involving Hamada coordinates, expressions are usually needed for the metric tensor elements (g_{ij}) and the spatial coordinates (R, Y, ϕ) as functions of the Hamada coordinates (V, θ, ζ). For example, in computation of saturated tearing mode amplitudes in axisymmetric toroidal equilibria [9], the poloidal Fourier harmonics of the metric tensor elements, as functions of the Hamada coordinates, are needed with enough accuracy to resolve fine details of the background pressure and current profiles, which are functions of V alone. With this type of application in mind, we have developed and implemented a direct method of finding Hamada coordinates in axisymmetric MHD equilibria. The problem is reduced to the solution of ordinary differential equations for the poloidal Fourier harmonics of R and Y and the components of the magnetic field as functions of the Hamada coordinate V. By using an adaptive ordinary differential equation solver, the accuracy and resolution in V can be adjusted as needed. The metric tensor elements can then be obtained directly.

To define Hamada coordinates (V, θ, ζ), consider a static, scalar pressure MHD equilibrium

$$\nabla p = \mathbf{J} \times \mathbf{B}, \tag{1}$$

$$\mu_0 \mathbf{J} = \nabla \times \mathbf{B}, \tag{2}$$

$$\nabla \cdot \mathbf{B} = 0, \tag{3}$$

in which the magnetic field lines lie on a simply nested set of toroidal surfaces, called magnetic surfaces. Let coordinate V be a surface quantity (uniform over each magnetic surface) which increases monotonically from the magnetic axis outward, so V can be used to label magnetic surfaces. Any such surface quantity will do, but we will make a convenient specific choice later in this paper. Let θ be an angle-like variable which increases by 2π the short way around the toroid, while ζ is an angle-like variable which increases by 2π the long way around the toroid. For Hamada coordinates, the variables θ and ζ are chosen so that the Jacobian is a surface quantity,

$$\mathscr{J} \equiv (\nabla V \cdot \nabla \theta \times \nabla \zeta)^{-1} = \mathscr{J}(V), \tag{4}$$

and the contravariant components of both the magnetic field and current density are surface quantities :

$$\mathbf{B} = \mathscr{J}(V)\, B^{\theta}(V)\, \nabla \zeta \times \nabla V + \mathscr{J}(V)\, B^{\zeta}(V)\, \nabla V \times \nabla \theta, \tag{5}$$

$$\mathbf{J} = \mathscr{J}(V)\, J^{\theta}(V)\, \nabla \zeta \times \nabla V + \mathscr{J}(V)\, J^{\zeta}(V)\, \nabla V \times \nabla \theta. \tag{6}$$

It can be shown that these conditions (4)–(6) are all consistent with the equilibrium conditions [1–3] and, in general, there is enough freedom to satisfy these conditions in axisymmetric toroidal equilibria. In this paper, we will consider only axisymmetric equilibria, in which ζ is an ignorable coordinate.

2. Hamada Coordinate Equations

For axisymmetric toroidal equilibria, we seek expressions for the polar coordinates (R, Y, ϕ), where R is the major radius, Y the vertical position, and ϕ the toroidal angle, in terms of Hamada coordinates (V, θ, ζ)

$$R = R(\theta, V), \tag{7}$$

$$Y = Y(\theta, V), \tag{8}$$

$$\zeta = \phi + G(\theta, V). \tag{9}$$

Both ζ and ϕ are ignorable coordinates with period 2π. From $\nabla R = \hat{R}$, $\nabla Y = \hat{Y}$, and $\nabla\phi = \hat{\phi}/R$, it follows that

$$\nabla V = \left(\frac{\partial Y}{\partial\theta}\hat{R} - \frac{\partial R}{\partial\theta}\hat{Y}\right)\bigg/\left(\frac{\partial R}{\partial V}\frac{\partial Y}{\partial\theta} - \frac{\partial Y}{\partial V}\frac{\partial R}{\partial\theta}\right), \tag{10}$$

$$\nabla\theta = \left(-\frac{\partial Y}{\partial V}\hat{R} + \frac{\partial R}{\partial V}\hat{Y}\right)\bigg/\left(\frac{\partial R}{\partial V}\frac{\partial Y}{\partial\theta} - \frac{\partial Y}{\partial V}\frac{\partial R}{\partial\theta}\right), \tag{11}$$

$$\nabla\zeta = \frac{1}{R}\hat{\phi} + \frac{\partial G}{\partial V}\nabla V + \frac{\partial G}{\partial\theta}\nabla\theta, \tag{12}$$

and

$$\mathcal{J} \equiv (\nabla V\cdot\nabla\theta\times\nabla\zeta)^{-1} = R\left(\frac{\partial R}{\partial V}\frac{\partial Y}{\partial\theta} - \frac{\partial Y}{\partial V}\frac{\partial R}{\partial\theta}\right) = \mathcal{J}(V). \tag{13}$$

From Eq. (2), the contravariant components of the current density are

$$\mu_0\mathcal{J}(V)J^V = \frac{\partial B_\zeta}{\partial\theta} - \frac{\partial B_\theta}{\partial\zeta} = 0, \tag{14}$$

$$\mu_0\mathcal{J}(V)\,J^\theta(V) = \frac{\partial B_V}{\partial\zeta} - \frac{\partial B_\zeta}{\partial V}, \tag{15}$$

$$\mu_0\mathcal{J}(V)\,J^\zeta(V) = \frac{\partial B_\theta}{\partial V} - \frac{\partial B_V}{\partial\theta}. \tag{16}$$

Using $\partial/\partial\zeta = 0$, Eq. (14) implies that B_ζ is a surface quantity which can be shown to be proportional to the total poloidal current passing around the toroidal flux surface

$$B_\zeta = B_\zeta(V) = RB_\phi \equiv I(\psi), \tag{17}$$

where ψ is the stream function defined by

$$\mathbf{B} = \nabla\phi \times \nabla\psi + B_\phi\hat{\phi}. \tag{18}$$

Eq. (15) relates B_ζ to J^θ,

$$\mu_0 \mathscr{J}(V)\, J^\theta(V) = -\frac{\partial B_\zeta}{\partial V}. \tag{19}$$

Note,

$$\frac{d\psi}{dV} = \mathscr{J}(V)\, B^\theta(V), \tag{20}$$

and that $\Psi = 2\pi\psi$ is the poloidal flux.

In order to use Eq. (16) we need to relate the covariant components B_θ, B_V to the contravariant components B^θ, B^ζ by use of the metric tensor

$$\begin{aligned} g_{VV} &= |\nabla\theta \times \nabla\zeta|^2 \mathscr{J}^2 \\ &= \left|\frac{\partial R}{\partial V}\right|^2 + \left|\frac{\partial Y}{\partial V}\right|^2 + \left|\frac{\partial G}{\partial V}\right|^2 R^2, \end{aligned} \tag{21}$$

$$\begin{aligned} g_{\theta\theta} &= |\nabla\zeta \times \nabla V|^2 \mathscr{J}^2 \\ &= \left|\frac{\partial R}{\partial \theta}\right|^2 + \left|\frac{\partial Y}{\partial \theta}\right|^2 + \left|\frac{\partial G}{\partial \theta}\right|^2 R^2, \end{aligned} \tag{22}$$

$$\begin{aligned} g_{\theta V} = g_{V\theta} &= \nabla\theta \times \nabla\zeta \cdot \nabla\zeta \times \nabla V\, \mathscr{J}^2 \\ &= \frac{\partial R}{\partial V} \cdot \frac{\partial R}{\partial \theta} + \frac{\partial Y}{\partial V} \cdot \frac{\partial Y}{\partial \theta} + \frac{\partial G}{\partial V}\frac{\partial G}{\partial \theta} R^2, \end{aligned} \tag{23}$$

$$g_{\zeta\zeta} = |\nabla V \times \nabla\theta|^2 \mathscr{J}^2 = R^2, \tag{24}$$

$$\begin{aligned} g_{\theta\zeta} = g_{\zeta\theta} &= \nabla\zeta \times \nabla V \cdot \nabla V \times \nabla\theta\, \mathscr{J}^2 \\ &= -\frac{\partial G}{\partial \theta} R^2, \end{aligned} \tag{25}$$

$$\begin{aligned} g_{V\zeta} = g_{\zeta V} &= \nabla\theta \times \nabla\zeta \cdot \nabla V \times \nabla\theta\, \mathscr{J}^2 \\ &= -\frac{\partial G}{\partial V} R^2. \end{aligned} \tag{26}$$

Since B^V is identically zero, only five metric tensor elements are needed to relate (B_V, B_θ, B_ζ) to $(B^\theta(V), B^\zeta(V))$. Using

$$B_\zeta(V) = -\frac{\partial G}{\partial \theta} R^2 B^\theta(V) + R^2 B^\zeta(V) \tag{27}$$

we can show

$$B_\theta = \left(\left| \frac{\partial R}{\partial \theta} \right|^2 + \left| \frac{\partial Y}{\partial \theta} \right|^2 \right) B^\theta(V) - \frac{\partial G}{\partial \theta} B_\zeta(V), \tag{28}$$

$$B_V = \left(\frac{\partial R}{\partial \theta} \frac{\partial R}{\partial V} + \frac{\partial Y}{\partial \theta} \frac{\partial Y}{\partial V} \right) B^\theta(V) - \frac{\partial G}{\partial V} B_\zeta(V). \tag{29}$$

The equations needed for Hamada coordinates then follow from Eq. (16)

$$\frac{\partial}{\partial V} \left[\left(\left| \frac{\partial R}{\partial \theta} \right|^2 + \left| \frac{\partial Y}{\partial \theta} \right|^2 \right) B^\theta(V) \right] - \frac{\partial}{\partial \theta} \left[\frac{\partial R}{\partial \theta} \frac{\partial R}{\partial V} + \frac{\partial Y}{\partial \theta} \frac{\partial Y}{\partial V} \right] B^\theta(V)$$
$$= \frac{\partial G}{\partial \theta} \frac{\partial B_\zeta}{\partial V}(V) + \mu_0 J^\zeta(V) \mathscr{J}(V), \tag{30}$$

and from the condition that the Jacobian be a surface quantity

$$R \left(\frac{\partial Y}{\partial \theta} \frac{\partial R}{\partial V} - \frac{\partial R}{\partial V} \frac{\partial Y}{\partial V} \right) = \mathscr{J}(V). \tag{31}$$

Equations (19), (27), (30) and (31) determine R, Y, G, B^θ, B^ζ and B_ζ if $J^\zeta(V)$ and $J^\theta(V)$ are considered to be given functions of V. Dividing Eq. (27) by R^2 and taking a flux surface average

$$\langle \cdots \rangle \equiv \frac{1}{2\pi} \int_0^{2\pi} d\theta \cdots, \tag{32}$$

yields

$$B^\zeta(V) = \left\langle \frac{1}{R^2} \right\rangle B_\zeta(V). \tag{33}$$

Equation (27) can then be used to eliminate $G(\theta, V)$ from Eq. (30). The force balance equation (1) merely relates contravariant components of current and magnetic field to dp/dV

$$\mathscr{J}(V)(J^\theta(V) B^\zeta(V) - J^\zeta(V) B^\theta(V)) = \frac{\partial p}{\partial V}. \tag{34}$$

Equations (19), (20), (27) and (34) can be used to write the source term of Eq. (30) into the form commonly used in the Grad–Shafranov equation

$$\frac{\partial}{\partial V}\left[\left(\left|\frac{\partial R}{\partial \theta}\right|^2+\left|\frac{\partial Y}{\partial \theta}\right|^2\right)B^\theta(V)\right]-\frac{\partial}{\partial \theta}\left[\frac{\partial R}{\partial V}\frac{\partial R}{\partial \theta}+\frac{\partial Y}{\partial V}\frac{\partial Y}{\partial \theta}\right]B^\theta(V)$$
$$=-\mathscr{J}(V)\left[\mu_0 p'(\psi)+\frac{II'(\psi)}{R^2}\right]. \tag{35}$$

This is the appropriate equation to use, along with Eq. (20), when $p(\psi)$ and $I(\psi)$ are given functions either of ψ or the surface label V.

In many situations it is more convenient [17] to use the safety factor q, instead of the toroidal field function I, where

$$q(V)=\frac{B^\zeta(V)}{B^\theta(V)}=\frac{B_\zeta(V)\,\langle 1/R^2\rangle}{B^\theta(V)}. \tag{36}$$

Equation (36) can then be rearranged to the form

$$B^\theta\frac{\partial}{\partial V}\left[\left(\left|\frac{\partial R}{\partial \theta}\right|^2+\left|\frac{\partial Y}{\partial \theta}\right|^2\right)B^\theta(V)\right]-\frac{\partial}{\partial \theta}\left[\frac{\partial R}{\partial V}\frac{\partial R}{\partial \theta}+\frac{\partial Y}{\partial V}\frac{\partial Y}{\partial \theta}\right](B^\theta)^2+\frac{B_\zeta(V)}{R^2}\frac{\partial B_\zeta}{\partial V}$$
$$=-\mu_0 p'(V), \tag{37}$$

and Eq. (36) differentiated to give

$$\left\langle\frac{1}{R^2}\right\rangle\frac{\partial B_\zeta}{\partial V}-q(V)\frac{\partial B^\theta}{\partial V}-B_\zeta\left\langle\frac{\partial R}{\partial V}\Big/R^3\right\rangle=q'(V)B^\theta. \tag{38}$$

These two equations, along with Eqs. (31) and (20), can be integrated to give B_ζ (i.e., I), B^θ, R and Y when $p'(V)$ and $q(V)$ are prescribed functions of V, or, with some modifications, as functions of ψ.

3. Poloidal Harmonic Equations

In order to reduce appropriate sets of equations to a system of ordinary differential equations in V, which can be solved to an arbitrarily high degree of accuracy, we expand R, Y and G in poloidal Fourier harmonics

$$R(\theta, V)=\sum_{m=-\infty}^{\infty} R_m(V)e^{im\theta}, \tag{39}$$

$$Y(\theta, V)=\sum_{m=-\infty}^{\infty} iY_m(V)e^{im\theta}, \tag{40}$$

$$G(\theta, V)=\sum_{m=-\infty}^{\infty} iG_m(V)e^{im\theta}. \tag{41}$$

The Jacobian equation (31) can then be written either in the form of a triple convolution

$$\sum_{m=-\infty}^{\infty} \sum_{k=-\infty}^{\infty} mR_{n-m-k}[-Y_k R'_m(V) + R_k Y'_m(V)] = \mathscr{J}(V)\,\delta_{n,0} \tag{42}$$

or, by bringing $1/R$ to the right hand side of Eq. (31), in the simpler form of a two term convolution

$$\sum_{m=-\infty}^{\infty} m[-Y_m R'_{n-m}(V) + R_m Y'_{n-m}(V)] = \mathscr{J}(V)\left(\frac{1}{R}\right)_n. \tag{43}$$

In the latter case, the Fourier harmonics of $1/R(\theta, V)$ can be found either by Fast Fourier Transforms or by solving the system of linear equations resulting from the convolution of $(1/R(\theta, V))\, R(\theta, V) = 1$.

Fourier harmonics of the force balance equation (35), take the form

$$\begin{aligned}\sum_{m=-\infty}^{\infty} & m(2m-n)(R_m R'_{n-m} - Y_m Y'_{n-m})\, B^{\theta}(V) \\ & - m(n-m)(R_m R_{n-m} - Y_m Y_{n-m})\, B^{\theta\prime}(V) \\ & = -\mathscr{J}(V)\,\mu_0\, p'(\psi)\,\delta_{n,0} - \mathscr{J}(V)\, II'(\psi)\left(\frac{1}{R^2}\right)_n.\end{aligned} \tag{44}$$

If Eq. (35) were rewritten, with the factor R^2 multiplied through, before taking Fourier harmonics, the Fourier convolutions on the left-hand side of the resulting harmonic equation would be more complicated. The alternative of using R^2 rather than R as the choice of variable has yet to be fully explored but this does not seem to be a necessary refinement.

Equation (27) can be used to find the Fourier harmonics of G

$$G_m = \frac{1}{m}\left(\frac{1}{R^2}\right)_m \frac{B_\zeta(V)}{B^{\theta}(V)}, \qquad m \neq 0, \tag{45}$$

which are needed only for determination of the metric tensor elements $g_{\theta\zeta}$ and $g_{V\zeta}$.

If the plasma equilibrium shape has a reflection symmetry across the midplane, then the harmonic coefficients are real-valued and obey the conditions

$$R_{-m} = R_m, \qquad Y_{-m} = -Y_m, \qquad G_{-m} = -G_m. \tag{46}$$

The harmonic expansions can then be written

$$R(\theta, V) = R_0(V) + \sum_{m=1}^{\infty} 2R_m(V)\cos(m\theta), \tag{47}$$

$$Y(\theta, V) = \sum_{m=1}^{\infty} 2Y_m(V)\sin(m\theta), \tag{48}$$

$$G(\theta, V) = \sum_{m=1}^{\infty} 2G_m(V)\sin(m\theta). \tag{49}$$

Note the factors of 2, which makes this different from the notation used in Ref. [13]. Although this reflection symmetry, which is common in tokamaks, will be used as a matter of convenience in the rest of this paper, it is not essential to either the development or the implementation of the method presented.

For each set of given functions (J^θ, J^ζ or p', I or p', q) the appropriate transformed equations can be written as a set of first order equations, linear in the derivatives with respect to V. Our algorithm for the direct determination of Hamada coordinates consists of numerically transforming these equations (for example, Eqs. (43) and (44)) into the form

$$\frac{d}{dV} R_m(V) = S_{R_m}(R_0,..., R_M, Y_1,..., Y_M, B^\theta, B_\zeta) \qquad (m=0, 1,..., M), \tag{50}$$

$$\frac{d}{dV} Y_m(V) = S_{Y_m}(R_0,..., R_M, Y_1,..., Y_M, B^\theta, B_\zeta) \qquad (m=0, 1,..., M), \tag{51}$$

$$\frac{d}{dV} B^\theta(V) = S_{B^\theta}(R_0,..., R_M, Y_1,..., Y_M, B^\theta, B_\zeta), \tag{52}$$

$$\frac{d}{dV} B_\zeta(V) = S_{B_\zeta}(R_0,..., R_M, Y_1,..., Y_M, B^\theta, B_\zeta), \tag{53}$$

together with Eq. (20) at each step in the numerical integration of the equations.

If a sufficiently large number of harmonics are considered, any of several methods of truncating Eqs. (43) and (44) work about equally well. If only a few harmonics are considered, we have found it best to take $M+1$ Jacobian equations (43) and $M-1$ force balance equations (44), since this choice emphasizes the most dominant set of coefficients in the case of a nearly circular cross section plasma.

4. Near the Magnetic Axis

We have chosen to use a Jacobian with the form

$$\mathscr{J}(V) = CV, \tag{54}$$

where C is a constant which is proportional to the total volume of the plasma (in particular $C = \text{Volume}/(2\pi^2)$ if $0 \leqslant V \leqslant 1$ within the plasma). Other functional forms of V could be chosen for the Jacobian, including the original choice of a constant [1, 2]. However, the order of the singularity at $V=0$ may be changed and one would have to take this into account in carrying out the analysis below. With the choice, Eq. (54), for the Jacobian, the contravariant components of the magnetic field, B^θ and B^ζ, go to non-zero constants near the magnetic axis. In the circular cylinder limit, the variable V becomes proportional to the minor radius (not the volume). The equations (50)–(53) have a singular point at $V=0$ and they are integrated outwards from a very small value of $V=\delta V$. However, with arbitrarily chosen starting values of $R_m(\delta V)$ ($m=0,..., M$), $Y_m(\delta V)$ ($m=1,..., M$), $B^\theta(\delta V)$ and $B^\zeta(\delta V)$, one may obtain solutions which are not acceptable physically. This occurs partly because the Jacobian will be determined by a choice of all the R_m's and the Y_m's. It is important therefore to constrain the choice of starting values so that these unacceptable solutions are eliminated. Physically reasonable solutions are those for which, near the magnetic axis ($V\sim 0$),

$$R_m(V)\sim V^{|m|} \tag{55}$$

and

$$Y_m(V)\sim V^{|m|} \tag{56}$$

(see Ref. [13]). As a first step it is useful to scale these variables and set up the set of equations (50) and (51) as differential equations for the variables $r_m(V)$ and $y_m(V)$, defined via

$$R_m(V)=V^{|m|}r_m(V) \tag{57}$$

and

$$Y_m(V)=V^{|m|}y_m(V) \tag{58}$$

and to look for solutions for which the r_m's and y_m's are approximately constant near $V=0$. In practice this scaling assists in maintaining numerical accuracy since $r_m(V)$ and $y_m(V)$ only vary slowly over the whole of the integration interval.

In order to illustrate the problem in a special case, consider the truncation of Eq. (50)–(52) with $M=1$ for the simple case where $J^\zeta(V)=J^\zeta=$ constant and $J^\theta(V)=0$. Near $V=0$, the truncated equations are

$$2Y_1\frac{\partial R_1}{\partial V}+2R_1\frac{\partial Y_1}{\partial V}=CV/R_0, \tag{59}$$

$$Y_1\frac{\partial R_0}{\partial V}=0, \tag{60}$$

$$Y_1\frac{\partial R_1}{\partial V}-R_1\frac{\partial Y_1}{\partial V}=0, \tag{61}$$

$$2\frac{d}{dV}((R_1^2+Y_1^2)\,B^\theta)=\mu_0 J^\zeta CV, \tag{62}$$

and $B_\zeta=$ constant.

With the change of dependent variables, Eqs. (57) and (58), these can be rearranged as

$$\frac{dr_0}{dV}=0, \tag{63}$$

$$\frac{dr_1}{dV}=\left(\frac{C-4r_0r_1y_1}{4r_0y_1V}\right), \tag{64}$$

$$\frac{dy_1}{dV}=\left(\frac{C-4r_0r_1y_1}{4r_0r_1V}\right), \tag{65}$$

$$\frac{dB^\theta}{dV}=\left(\frac{\mu_0J^\zeta C}{2r_0(r_1^2+y_1^2)}-2B^\theta\right)\Bigg/V-\frac{(C-4r_0r_1y_1)}{2r_0(r_1^2+y_1^2)V}B^\theta\left(\frac{r_1}{y_1}+\frac{y_1}{r_1}\right). \tag{66}$$

Solutions of these equations near $V=0$ for which r_0, r_1, y_1 and $B^\theta \sim$ constant are only possible if the constraints

$$4r_0r_1y_1=C \tag{67}$$

and

$$B^\theta=\frac{\mu_0J^\zeta C}{4r_0(r_1^2+y_1^2)} \tag{68}$$

are satisfied at $V=0$, by the appropriate choice of, e.g., y_1 and B^θ or by the choice of B^θ and the constant C. If these constraints are satisfied the solution of Eqs. (63)–(66) corresponds to a straight elliptical plasma column with $R=r_0+r_1V\cos\theta$, $Y=y_1V\sin\theta$ and $B^\theta=$ constant (r_0, r_1, y_1 constant).

The REDUCE computer program [18] was used to analyse the general set of equations for larger numbers of Fourier harmonics and it was shown that the singular behaviour can be eliminated in general by introducing further constraints. However, for increasing M, these rapidly become intractable and there appears to be no systematic algorithm to impose the constraints analytically. In practice, therefore, the constraints are imposed numerically by choosing $r_0, r_1, \ldots, r_M$ and y_1 for an arbitrarily small value of δV and then searching for values of $y_2, \ldots, y_M$, B^θ and C which minimize sngular behaviour. The conditions used, that the sum of the squares of the derivatives of $r_0, r_1, \ldots, r_m$, $y_1, \ldots, y_m$ and B^θ are minimized, effectively eliminate the singularities. It was noted, in addition, that if values of the y's, etc., are chosen which do not satisfy the constraint conditions, then the differential equation solutions undergo a rapid transient and then integrate smoothly outward. For larger values of V these solutions differ only slightly from the solutions for which the constraints were applied. Thus the overall numerical error in the solutions for which the constraint conditions are not exactly satisfied is in practice very small.

Analysis of the origin of one of the constraint equations gives some insight to the relationship between the Fourier harmonics of $R(\theta)$ and $Y(\theta)$ and the parameter C. If the variable V is chosen to be in the range (0, 1) in the plasma, then

$$\text{Plasma volume} = (2\pi)^2 \int_0^1 \mathscr{J}(V)\, dV$$
$$= (2\pi)^2\, C/2. \tag{69}$$

Alternatively,

$$\text{Plasma volume} = (2\pi) \iint_{\text{plasma}} R\, dR\, dY$$
$$= (2\pi) \int_0^{2\pi} R(\theta)\, Y(\theta) \frac{dR(\theta)}{d\theta}\, d\theta, \tag{70}$$

i.e.,

$$C = \frac{2}{\pi} \int_0^{\pi} R(\theta)\, Y(\theta) \frac{dR(\theta)}{d\theta}\, d\theta. \tag{71}$$

This is to be equivalent to Eq. (67) when the Fourier series for $R(\theta)$ and $Y(\theta)$ are truncated at $M=1$. Using C, rather than y_1, as one of the variables used to satisfy the constraints enables us to automatically choose the scaling of V so that $V=1$ on the plasma surface.

5. Matching the Outer Shape of the Plasma

Any solution of Eqs. (50)–(53) which satisfies the constraints at $V \sim 0$ represents a plasma equilibrium in Hamada coordinates. In order to find a particular equilibrium, however, it is frequently desirable to be able to prescribe the shape of the outer (or any internal) boundary of the plasma. It is not clear how to do this directly with Hamada coordinates, but we have devised an indirect method which makes use of a polar coordinate representation of the boundary.

Consider a representation of a cross section of the boundary around its geometric centre at $(R, Y) = (R_p, 0)$

$$\rho = \rho_p(\theta_p), \tag{72}$$

where θ_p is a polar angle around R_p and $\rho_p(\theta_p)$ is a prescribed function for the minor radius from R_p to the boundary (Fig. 1). At any stage in the iteration over Hamada coordinates we have R and Y as functions of the Hamada angle θ at the outer boundary $V=1$, $R_H(\theta)$, $Y_H(\theta)$, which result from the integration of Eqs. (50)–(53) with some choice of initial conditions.

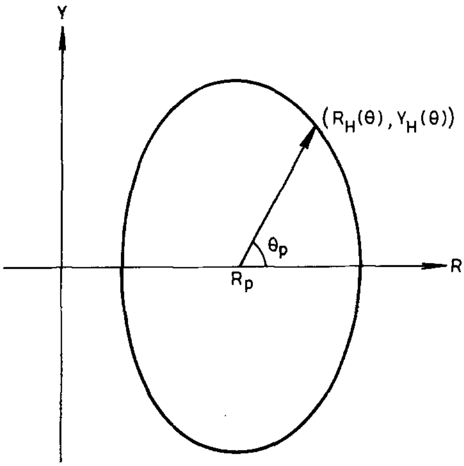

FIG. 1. Polar coordinate representation for the boundary of the plasma.

From geometrical considerations, we can determine the polar angle and minor radius as a function of Hamada angle at any point along the boundary of the solution to the Hamada equations

$$\tan \theta_p = \frac{Y_H(\theta)}{R_H(\theta) - R_p} \tag{73}$$

$$\rho_H^2 = (R_H(\theta) - R_p)^2 + Y_H^2(\theta). \tag{74}$$

We can then vary the $M+2$ free initial parameters in the solution of the Hamada equations in order to minimize the average distance between ρ_H and ρ_p. That is, we can minimize

$$\| \rho_H(\theta) - \rho_p(\theta_p(\theta)) \|, \tag{75}$$

where $\| \cdots \|$ is any reasonable choice of global norm. In particular, we have chosen to minimize the absolute value of the area between the prescibed and the Hamada boundary curves

$$\int_0^{2\pi} d\theta_p \, | \rho_H^2 - \rho_p^2 |. \tag{76}$$

In principle, any shape (including indented boundaries) can be matched provided that the function $\rho_p(\theta_p)$ is single-valued. A major modification would, however, be requred to treat situations where the plasma shape is determined by currents in external coils.

6. Verification and Results

The algorithm has been coded and tested by comparing the results of the code with the exact equilibrium of Solev'ev [17, 19] for constant values of $dp/d\psi$ and I. For this equilibrium

$$\Psi_s = \frac{A}{2\pi}\left[Y^2(R^2 - B) + \frac{E^2}{4}(R^2 - R_s^2)^2 \right], \tag{77}$$

the parameters A, B, E and R_s being constants. R_s is the position of the magnetic axis and E is the ellipticity in the vicinity of the magnetic axis. The outer shape of the plasma was defined, as in Section 5, by specifying it in terms of the calculated Fourier coefficients (with respect to the polar angle) of the polar distance from an interior point (chosen at approximately the centre).

The result from the code, Ψ_H, was then compared with Ψ_s by calculating the relative error averaged over a number N_s flux surfaces and M_s Hamada poloidal angles θ:

$$\varepsilon = \frac{\sum_{i=1}^{N_s} \sum_{j=1}^{M_s} |\Psi_H(V_i) - \Psi_s(R(V_i, \theta_j), Y(V_i, \theta_j))|}{N_s M_s |\psi_H(1) - \Psi_H(\delta V)|}. \tag{78}$$

In addition the calculated position of the magnetic axis R_0 was compared with the analytic value. This was done for various numbers, M, of Fourier harmonics used in the specification of R and Y. Results for a typical comparison are given in Table I. These results are for the case for which $A = 0.34906$, $B = 0$, $E = 1.0$, and $R_s = 3.0$ and the average is taken over $M_s \times N_s = 32 \times 10$ points.

Figure 2 shows graphs of the reduced Fourier coefficients for this case. These show that the convergence of the Fourier series is fast and that the variation of the Fourier coefficients across the plasma is considerably reduced by the scaling of Eq. (57) and (58). The code is very fast and a single outward integration of the equations (with $M = 4$ and a specified relative error of 10^{-5} for the integration subroutine takes approximately 14 sec on the Flinders University Prime-750. The

TABLE I

Number of Fourier components	Average relative error	Position of magnetic axis
M	ε	R_0
1	0.0347	2.9403
2	0.0034	2.9971
3	0.0006	2.9999
4	0.0007	2.9998
		(exact 3.0000)

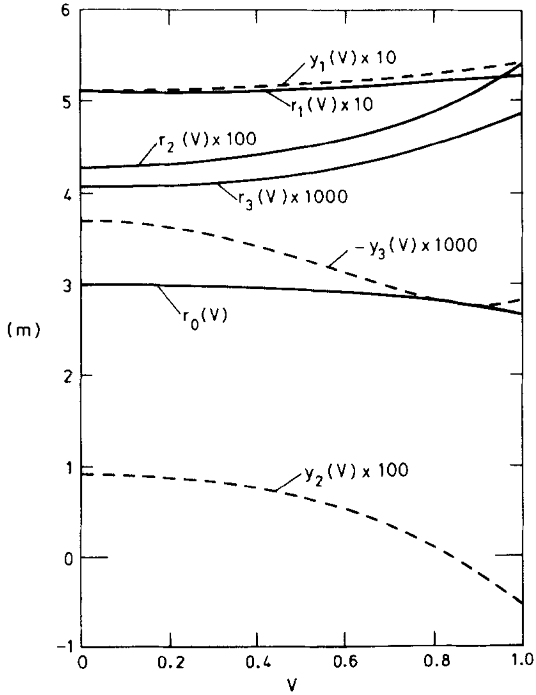

FIG. 2. Reduced Fourier coefficients as a function of the Hamada flux coordinate V for a Solev'ev equilibrium.

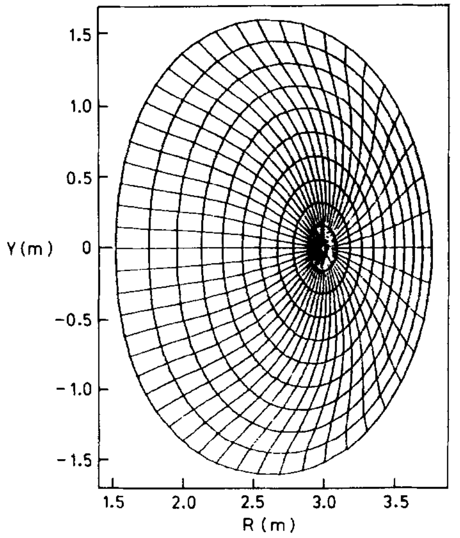

FIG. 3. A high-beta ($\beta \sim 17\%$), low aspect ratio equilibrium ($q_{axis} = 1.0$, $q_{edge} = 3.0$) obtained using this algorithm.

parameter search for this case to fit the outer boundary took between 11 and 30 integrations, depending on M and the accuracy required. This is in contrast to the time required to obtain an equilibrium using the iteration procedure of Ref. [17] and to carry out the flux coordinate mapping as in Ref. [10]. An increase in time of at least a factor of 10 would be required and in some cases (for a large number of required flux surfaces) this could increase to a factor nearer 100.

An example is presented in Fig. 3 of the calculation of a high-beta ($\beta \sim 17\%$) equilibrium at a relatively low aspect ratio (~ 3) for a plasma with an approximately elliptical surface. For this case the safety factor q was specified with $q(V) = 1.0 + 2.0\, V^2$ $(0 \leqslant V \leqslant 1)$. This case was calculated with the number of Fourier coefficients, $M = 4$. This equilibrium, which was obtained by specifying $R_0 = 3.0$, $R_1 = 0.5$, $Y_1 = 0.8$, $R_2 = 0.03$ and $R_3 = 0.03$ near the magnetic axis, is fairly sensitive to these Fourier coefficients. For example, a charge of R_3 to 0.02 will produce a very much more D-shaped plasma.

Acknowledgments

The authors acknowledge the support of the Australian Research Grants Scheme and the Flinders University Visiting Research Fellowship Scheme. We also wish to thank Mr. C. Lennard for assistance with the computing aspects of the paper.

References

1. S. Hamada, *Nuclear Fusion* **2** (1962), 23.
2. J. M. Greene and J. L. Johnson, *Phys. Fluids* **5** (1962), 510.
3. G. Bateman, "MHD Instabilities," MIT Press, Cambridge, Mass, 1978.
4. C. Mercier and H. Luc, "The MHD Approach to the Problem of Plasma Confinement in Closed Magnetic Configurations," EUR 5127e, Commission of the European Communities, Luxembourg, 1974.
5. D. Dobrott, D. B. Nelson, J. M. Greene, A. H. Glasser, M. S. Chance, and E. A. Frieman, *Phys. Rev. Lett.* **39** (1977), 943.
6. A. H. Glasser, "Ballooning Modes in Axisymmetric Toroidal Plasmas," Lectures presented at the Princeton Plasma Physics Laboratory 1978 (unpublished).
7. A. H. Glasser, J. M. Greene, and J. L. Johnson, *Phys. Fluids* **18** (1975), 875.
8. A. B. Mikhailovskii, *Nuclear Fusion* **15** (1975), 95.
9. G. Bateman and R. H. Morris, Georgia Tech. Fusion Report GRFR-31, 1982 (unpublished).
10. R. C. Grimm, J. M. Greene, and J. L. Johnson, *in* "Methods in Computational Physics" Vol. 16, p. 253, Academic Press, New York, 1976.
11. R. Gruber, F. Troyon, D. Berger, L. C. Bernard, S. Rousset, R. Schreiber, W. Kerner, W. Schneider, and K. V. Roberts, *Comput. Phys. Commun.* **21** (1981), 323.
12. J. DeLucia, S. C. Jardin, and A. M. M. Todd, *J. Comput. Phys.* **37** (1980), 183.
13. L. L. Lao, S. P. Hirshman, and R. M. Wieland, *Phys. Fluids* **24** (1981), 1431.
14. S. P. Hirshman and J. C. Whitson, *Phys. Fluids* **26** (1983), 3553.
15. V. D. Khait, *Fiz. Plazmy* **6** (1980), 871 (*Soviet J. Plasma Phys.* **6** (1980), 476).
16. R. C. Grimm, R. L. Dewar, and J. Manickam, *J. Comput. Phys.* **49** (1983), 94.

17. J. L. Johnson, H. E. Dalhed, J. M. Greene, R. C. Grimm, Y. Y. Hsieh, S. C. Jardin, J. Manickam, M. Okabayashi, R. G. Storer, A. M. M. Todd, D. E. Voss, and K. E. Weimer, *J. Comput. Phys.* **32** (1979), 212.
18. A. C. Hearn, "REDUCE 2," University of Utah report UCP-19, 1973 (unpublished).
19. L. S. Solev'ev, *Z. Eksper. Teor. Fiz.* **53** (1967), 626 (*Soviet Phys. JETP* **26** (1968), 400).
20. A. Bhattacharjee, J. C. Wiley, and R. L. Dewar, *Comput. Phys. Commun.* **31** (1984), 213.